Electron beam induced electronic transport in alkyl amine-intercalated VO_x nanotubes

C. O'Dwyer[*1], **V. Lavayen**[2], **C. Clavijo-Cedeño**[3], and **C. M. Sotomayor Torres**[4,5]

[1] Department of Physics, and Materials and Surface Science Institute, University of Limerick, Limerick, Ireland
[2] UFMG, Departamento de Física, Av. Antônio Carlos, 6627, Belo Horizonte, 30123-970, MG, Brazil
[3] Department of Mathematics and Computer Science, University of Twente, The Netherlands
[4] Institute for Research and Advanced Studies, ICREA, 08010 Barcelona, Spain
[5] Catalan Institute of Nanotechnology, Edifici CM7, Campus Universitat Autonoma de Barcelona, 08193 Bellaterra (Barcelona), Spain

Received zzz, revised zzz, accepted zzz
Published online zzz

PACS 73.22.-f, 73.63.-b, 81.07.-b, 85.30.-z, 72.60.+g, 61.46.+w

The electron beam induced electronic transport in primary alkyl amine-intercalated V_2O_5 nanotubes is investigated where the organic amine molecules are employed as molecular conductive wires to an aminosilanized substrate surface and contacted to Au interdigitated electrode contacts. The results demonstrate that the high conductivity of the nanotubes is related to the non-resonant tunnelling through the amine molecules and a reduced polaron hopping conduction through the vanadium oxide itself. Both nanotube networks and individual nanotubes exhibit similarly high conductivities where the minority carrier transport is bias dependent and nanotube diameter invariant.

1 Introduction

Molecular electronics is foreseen to be a viable alternative for inorganic semiconductor circuitry [1,2] where a drive to develop cost-efficient and reproducible techniques to facilitate the demands of the low dimensionalities required in the next-generation devices [3,4]. Desirable properties will depend on the ability to realize functional nanostructures with controllable and superior electronic properties and the ability to withstand high current densities [5]. Low-dimensional nanostructures, such as chemically synthesized nanowires or nanotubes [6,7], are of considerable interest as functional units mediating the transport of electrons or optical excitations.

Here we present the controlled deposition and electrical properties of alkyl amine-intercalated VO_x nanotubes. The findings comprise the fabrication of processable hybrid organic-inorganic VO_x-nanotube conductive channel contacts and the determination of the electronic transport characteristics of the hybrid organic-inorganic nanotubes compared to those employing vanadate wires or ribbons, by an electron beam induced current methodology.

2 Experimental

The synthesis of primary alkyl amine intercalated VO_x nanotubes by hydrothermal methods has been outlined in detail elsewhere [8,9]. Briefly, VO_x nanotubes intercalated with monoamines (octade-

[*] Corresponding author: e-mail: colm.odwyer@ul.ie, Phone: +353 61 202288, Fax: +353 61 213529

cylamine) were deposited on patterned device areas from a suspension in octanol. The substrates were gold electrodes on SiO_2. Utilizing the negative surface charge, individual VO_x nanotubes can be deposited onto appropriately modified Si/SiO_2 surfaces. For that purpose, the SiO_2 surface is first treated with 3-aminopropyltriethoxysilane (3-APS) to create positively charged ammonium groups on the surface. The ionic interaction then allows a controlled adsorption process [10]. Deposition of only a few single VO_x nanotubes was achieved by optimization of the sol concentration (~10^{-3} mol dm^{-3}) and adsorption time (<5 s). The sub-micrometer channel length interdigitated electrodes (IDEs) were patterned by nanoimprint lithography (NIL) with an OBDUCAT Nanoimprinter giving metal stamps containing interdigitated electrodes (IDEs) with parallel lines of controllable spacing. Specific details on the imprinting methodology can be found elsewhere [11,12].

Electrical properties were investigated in the direct current (DC) regime using a Keithley Model 6517A Electrometer. Sample devices to be characterized were packaged in a Kryocera 16 LD S/B chip carrier and wire bonded with gold wires using F&K Delvotec Bondtechnik ultrasound ballbonder 5405. Additionally, the complementary technique of electron beam induced current (EBIC) was used to gauge the electronic transport in VO_x nanotubes that were both bonded and sol deposited, and performed in a Hitachi S-2500 SEM using a Matelect ISM-5 system for signal detection. The induced current was recorded as a function of the position of a focused electron beam using a lock-in amplifier and an electron beam modulated at 1.2 kHz by the beam blanker.

3 Results and discussion

Figure 1a shows the typical NIL processed IDEs. Such device areas can have inter-electrode spacing ranging from several µm down to 50 nm. The IDE spacing in Fig. 1a is 100 nm. Solution deposited nanotube networks were deposited on the aminosilanized substrates using absorption times of several minutes at sol concentrations <0.03 mol dm^{-3} in octanol. Figure 1b shows a standard topological image of the nanowire network. The room temperature I-V response of VO_x nanotubes on an IDE with 100 nm inter-electrode spacing is shown in Fig. 1c, and exhibits nonlinear and symmetric I-V characteristics. A contact resistance of 0.47-0.98 kΩ was derived by comparison between 2- and 4-probe measurements on various nanotube network deposits. Since the effective cross-section of the samples is known (variable with nanotube feature size), the corresponding conductivity ranges from 0.2 – 0.8 S cm^{-1} at 300 K.

The conduction mechanism of vanadium oxide is generally accepted to be the hopping of electrons between the transition-metal ions in different valence states (V^{4+} and V^{5+}). These charge carriers are actually small polarons. As the electron-phonon coupling is considerable, the 3*d* unpaired electrons are trapped in their own polarization wells. Depending on the preparation method, the amount of V^{4+} can vary; we previously determined that for nanotubes used in this work [13], V^{4+} constitutes ~45% of the total quantity of vanadium atoms in the sample which is an order of magnitude greater that that typically found in V_2O_5 sols [14].

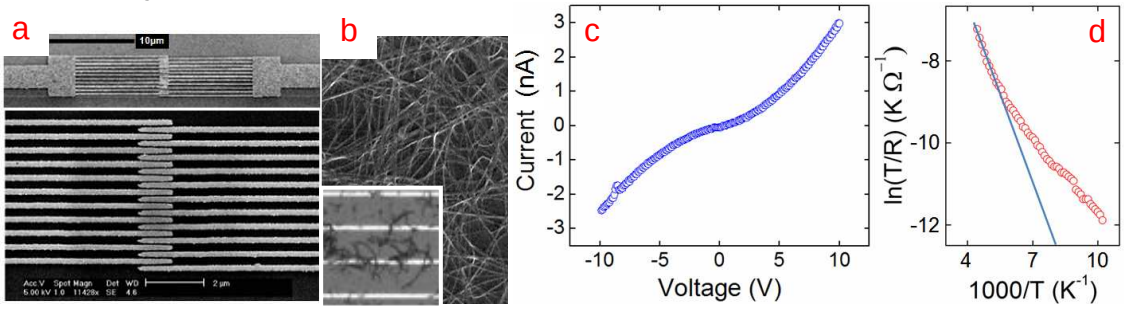

Fig. 1 (a) SEM images of IDEs fabricated by NIL with channel lengths of 100 nm. Scale bars = 10 µm (*top*) and 2 µm (*bottom*). (b) SEM image of the solution deposited VO_x nanotube network (*inset*) the nanotubes spread across several metal fingers. (c) I-V curve of the VO_x nanotube network on the interdigitated active area at room temperature. (d) Temperature dependence of the nanotube network resistance of the same sample area measured in (c).

Temperature dependent measurements revealed a decline in conductivity with decreasing temperature, consistent with thermally activated hopping transport. The resistance R of the deposited nanotube network is plotted in Fig. 1d as $\ln(T/R)$ versus reciprocal temperature in the range of 100 – 300 K. This plot is performed to analyze the data in the frame of the general formula proposed by Mott [15] for small polaron hopping in transition metal oxides:

$$\sigma = \left(\frac{\nu_0 e^2 C(1-C)}{kTr} \right) e^{(-2\alpha r)} e^{\left(\frac{-E_a}{kT}\right)}$$

where ν_0 is the phonon frequency, C the concentration ratio $V^{4+}/(V^{4+} + V^{5+})$ representing the fraction of sites occupied by electrons or polarons, or the ratio of the transition-metal ion concentration in the lower valency state to the total concentration (C = 0.45 in this case [13]), r the average hopping distance, E_a the activation energy, and α is the rate of wave function decay. The nanotube walls are composed of vanadium oxo-anions with either a neutral or negative charge. The presence of V^{5+} neutralizes this charge if present; V^{4+} does not. Consequently, the total anion charge on the nanotube walls is a direct function of the V^{4+} content. As the amine surfactant used in this work is the structural template and also cationic, greater quantities of V^{4+} results in an increased amount of surfactant binding as the associated electrostatic interaction is much stronger than dative bonding between neutral V^{5+} sites and amine head groups [16].

The nonlinearity of the $\ln(T/R)$ as a function of inverse temperature in Fig. 1d is in agreement with previous observations [17]. This behaviour has been explained by the temperature dependence of the hopping activation energy E_a, which includes a disorder energy contribution attributed to the random structure of the material which in previous cases arose from thick sol-gel samples. Approximating the data in Fig. 1d by a straight line in the temperature range 170 – 300 K gives an activation energy of 0.138 eV. This value is significantly lower than previous reports for entangled nanowire networks of V_2O_5 and comparable to values reported for individual V_2O_5 nanowire contacts. The reason is two-fold: firstly, even though the nanotubes are entangled in a dispersed array, each atomic layer of vanadium oxide is effectively sandwiched between monolayers of conducting amines [18] which form a conductive organic sheath around the metal oxide, improving intra-tube transport compared to monolithic V_2O_5 nanowires. Secondly, the smaller polaron hopping activation energy, reflecting the absence of significant transport barriers at the nanotube contacts, is also facilitated by interaction of conductive amine molecules. Indeed the conductivity of these nanotube networks (0.2 – 0.8 S cm^{-1}) matches and exceeds that of single V_2O_5 nanowires (~0.5 S cm^{-1}) [19]. Thus, the amine intercalated nanotubes comprise an alternative to complicated selective ordering steps associated with pure nanowires, due to the beneficial molecular conduction provided by the intercalated organic monolayers between every second layer of vanadium oxide, discussed further on.

EBIC measurements were conducted on individual as well as a network of organic-inorganic nanotubes in order to map the conductivity and electronic transport through the tubes and specifically at their contact point to the metal fingers of the IDEs. VO_x nanotubes were drop cast across the IDE, shown in Fig. 2a. Devices were loaded into a scanning electron microscope (SEM) in which a focused electron beam was scanned over the nanowire contacts while changes in current were measured as a function of the beam position. Voltage contrast resolution is the same as for secondary electron imaging. Hence for an acceleration voltage of 30 kV, a resolution of about 20 nm may be expected. However, for thin specimen such as a VO_x nanotube (~50 nm, perpendicular to the tubes long axis), a 30 kV beam only weakly interacts with the sample. Lower voltages between 0.5 – 5 kV allow sufficient sample-beam interaction. For voltages <1 kV and beam currents under 1 pA, we observed negligible degradation of the EBIC. Secondary electron and corresponding EBIC images of the nanotube contacted electrodes can be seen in Fig. 2b where we observe a uniform intensity representing metal-nanotube-metal current flow. The height of the conductive channel was determined to be ~50 nm, and is similar to the cross-sectional diameter of a single nanotube. The n-type nanotube was reverse biased to analyse the carrier kinetics at both contacts. For the Schottky contact, the energetic electron beam locally generates excess minority carriers (holes), which diffuse in the nanowire channel and are collected if they reach the contact before

recombining. The resolution for EBIC measurements is ~30 nm for VO_x nanotube-covered IDEs. Using voltages up to 1 kV and beam currents up to 1 pA, VO_x nanotubes did not exhibit measurable current degradation through the nanotubes. For voltages of 20 kV and beam currents of 150 pA, the conductivity of the nanotubes was observed to increase by one order of magnitude. The I-V characteristics (not shown) of a single organic-inorganic nanotube-contacted between two metal fingers of the IDE exhibit a linear I-V plot, confirming the advantageous conduction effect of the intercalated amines: we observed an increased conductivity (0.8 S cm^{-1}) and a much lower ohmic resistance of 2.4 kΩ, an order of magnitude improvement over monocrystalline nanofibers of V_2O_5 with a Au-Pd overlayer to improve nanotube-metal contact quality [19].

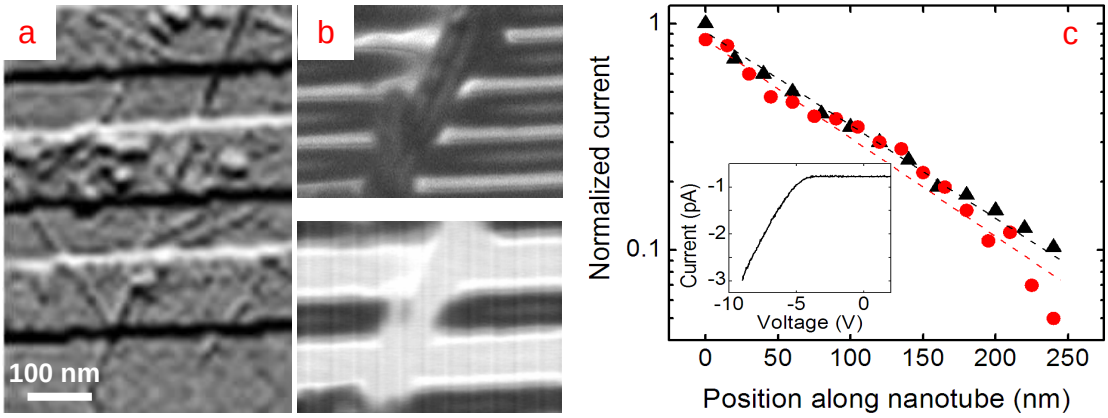

Fig. 2 (a) Non-contact AFM image of the solution-deposited VO_x nanotubes on an IDE. (b) Secondary electron image (*top*) and corresponding EBIC image (*bottom*) of nanotube-channelled electrode fingers. The electrode spacing is 100 nm. (c) Semi-logarithmic EBIC line profiles from a Schottky contact at 5 kV for nanotube diameters of (•) 75 nm (▲) 200 nm. (*Inset*) I-V curve of the reverse bias nanotube-electrode contact.

The increase in conductivity compared to the network of nanotubes (shown in Fig. 1) is directly due to an increase in carrier concentration caused by the non-resonant tunnelling through intercalated amines [20], a reduced polaron hopping activation energy in the VO_x and a reduction in carrier depletion at the nanotube-electrode contact. We analyzed the minority carrier diffusion length by monitoring the rate of decay of the EBIC along the nanotube long-axis and at the electrode contact, for two nanotubes of diameters 75 nm and 200 nm, respectively, at their respective Schottky contacts to the Au electrodes. Figure 2c shows that the EBIC decay constant of the exponential does not change with accelerating voltage (2 – 8 kV) but does so considerably with potential bias indicating a dependence of the minority carrier transport on the electric field within the electrodes. The dashed lines in Fig. 2c are fits to the current along the nanotube, which decays as $\alpha e^{(-x/Lp)}$, where L_p is the minority carrier diffusion length and x is the distance along the nanotube. From the data in Fig. 2c, the minority carrier diffusion lengths were determined to be 80 ± 7 nm and 91 ± 8 nm for nanotubes of diameters of 200 nm and 75 nm respectively. Such low values of L_p are essentially diameter invariant and are observed to remain in the range 80 – 100 nm for all nanotube diameters investigated (50 – 400 nm).

EBIC analysis of the Schottky contact between the amine-intercalated nanotube and the Au electrode of the IDE was conducted using a two terminal n-type VO_x nanotube diode. Figure 3a shows an SEM image of the actual contact point with the associated EBIC image in Fig. 3b. The EBIC was acquired along and perpendicular to the nanotube axis and is reproduced in Fig. 3c. The abrupt drop-off of the signal away from the nanotube confirms that backscattered electrons do not contribute to the signal. Of importance is that the minority carriers are collected at the contact before recombining. Some of the variation of the minority carrier diffusion length may be due to the fact that surface band bending exercises less influence over carriers generated in the middle of the nanotube as the diameter increases.

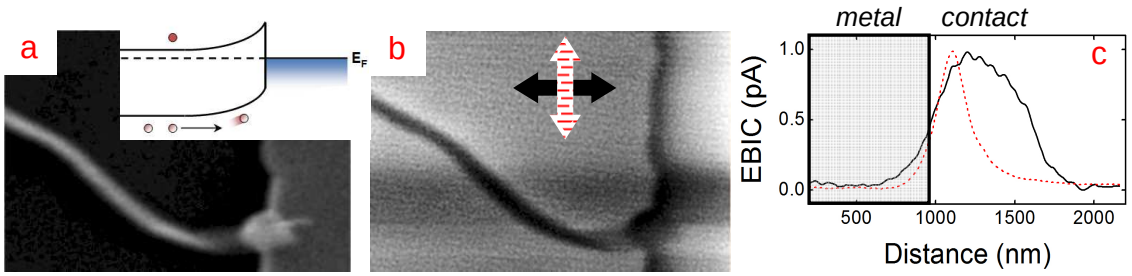

Fig. 3 (a) Secondary electron and (b) EBIC images of a single VO_x nanotube Schottky contact to a Au metal electrode. (*Inset (a)*) Band diagram where excess minority carriers diffuse to the space charge region and are swept to the contact by the internal electric field. (c) Line profiles of the data in (b) taken along (solid line/black arrow) and perpendicular (dashed line/dashed arrow) to the nanotube axis showing the signal decay.

Since VO_x nanotubes are scrolls of stacked double bilayers [8,18] with a hollow core, all transport occurs away from the tube center. Recombination at either amine structural defects or ionized impurity centers in the vanadium oxide limits the hole diffusion length, confirming the invariance of the reverse bias I-V characteristics with nanotube diameter. In addition, since L_p does not vary with nanotube diameter, the implication is that the surface recombination velocity is not constant. The reduced resistance routinely observed with an amine/Au contact is ascribed to differences in charge transfer and wave function mixing at the metal/molecule contact, including effects of nitrogen lone pair interaction with the gold which result in a hybrid wave function directed along the molecule bond axis. The details of the specific amine/Au conductive molecular junction will be presented elsewhere.

The findings serve as an important reminder that for semiconductor nanomaterials, control over the surface chemistry is at least as important as control over the bulk chemical properties, particularly in hybrid organic-inorganic nanostructures. For nanomaterials employed in next-generation photovoltaics, for example, it is prudent to be able to vary and control the minority carrier diffusion length in structures utilized in devices to avoid compromising their performance.

4 Conclusions

In summary, we have synthesized vanadium oxide nanowire networks via polycondensation on metallic interdigitated electrode devices and investigated the minority carrier transport properties and electronic conduction. The electrical transport was explained by the small polaron theory, employing the multi-optical-phonon-assisted hopping model at high (>180 K) temperatures. Compared to the nanotube networks, the individual nanotubes are characterized by a reduced hopping activation energy, reflecting the absence of transport barriers at the inter-tube contacts by conduction facilitated by non-resonant charge tunnelling through intercalated amine molecules at the contact point. Minority carrier diffusion is observed to be controlled by the variable surface recombination velocity within the hybrid organic-polyvalent nanotube material and the minority carrier diffusion length is nanotube diameter invariant.

Acknowledgements This material is based upon work supported by the Science Foundation Ireland under Grant No. 02/IN.1/172. Support from the EU-Network of Excellence P*h*OREMOST (FP6/2003/IST/2-511616) is also gratefully acknowledged.

References

[1] S. J. Tans, A. R. M. Verschueren, C. Dekker, Nature **393**, 49 (1998).
[2] R. Martel, T. Schmidt, H. R. Shea, T. Hertel, P. Avouris, Appl. Phys. Lett. **73**, 2447 (1998).
[3] R. Tenne, L. Margulius, M. Genut, G. Hodes, Nature **360**, 444 (1992).
[4] S. J. Tans, M. H. Devoret, H. Dai, A. Thess, R. E. Smalley, L. J. Geerligs, C. Dekker, Nature **386**, 474 (1997).
[5] S. Frank, P. Poncharal, Z. L. Wang, W. A. de Heer, Science **280**, 1744 (1998).

[6] M. E. Spahr, P. Bitterli, R. Nesper, M. Müller, F. Krumeich, H. U. Nissen, Angew. Chem. Int. Ed. **37**, 1263 (1998).
[7] J. Livage, Coord. Chem. Rev. **178-180**, 999 (1998).
[8] C. O'Dwyer, D. Navas, V. Lavayen, E. Benavente, M. A. Santa Ana, G. González, S. B. Newcomb, C. M. Sotomayor Torres, Chem. Mater. **18**, 3016 (2006).
[9] G. R. Patzke, F. Krumeich, and R. Nesper, Angew. Chem. Int. Ed. **41**, 2446 (2002).
[10] G. T. Kim, J. Muster, V. Krstic, J.G. Park, Y.W. Park, S. Roth, M. Burghard, Appl. Phys. Lett. **76**, 1875 (2000).
[11] A. P. Kam, J. Seekamp, V. Solovyev, C. Clavijo Cedeno, A. Goldschmidt, C. M. Sotomayor Torres, Microelec. Eng. **73-74**, 809 (2004).
[12] C. Clavijo Cedeno, J. Seekamp, A. P. Kam, T. Hoffmann, S. Zankovych, C. M. Sotomayor Torres, C. Menozzi, M. Cavallini, M. Murgia, G. Ruani, F. Biscarini, M. Behl, R. Zentel, J. Ahopelto, Microelec. Eng. **61-62**, 25 (2002).
[13] C. O'Dwyer, M. A. Santa Ana, S. B. Newcomb, E. Benavente, G. González, C. Sotomayor Torres, phys. stat. sol. (b) **243**, 3285 (2006).
[14] N. Gharbi, C. Sanchez, J. Livage, J. Lemerle, L. Nejem, and J. Lefebvre, Inorg. Chem. **21**, 2758 (1982).
[15] N. F. Mott, J. Non-Cryst. Solids **1**, 1 (1968).
[16] V. Petkov, P. Y. Zavalij, S. Lutta, M. S. Whittingham, V. Paranov, S. Shastri, Phys. Rev. B **69**, 085410 (2004).
[17] J. Bullot, O. Gallais, M. Gauthier, J. Livage, Appl. Phys. Lett. **36**, 986 (1980).
[18] C. O'Dwyer, V. Lavayen, S. B. Newcomb, E. Benavente, M. A. Santa Ana, G. González, C. M. Sotomayor Torres, Electrochem. Solid-State Lett. **10**, A111 (2007).
[19] J. Muster, G.T. Kim, V. Krstic, J.G. Park, Y.W. Park, S. Roth, M. Burghard, Adv. Mater. **12**, 420 (2000).
[20] C. Chu, J.-S. Na, G. N. Parsons, J. Am. Chem. Soc. **129**, 2287 (2007).